A Dissertation on

Study of complete fusion and incomplete fusion processes in decay of $^{96}Tc^{*}$ nuclear system

Submitted towards the partial fulfillment for the

Requirements of the degree of

Master of Science

in

Physics

Submitted by

Neha Grover

Roll No-301104010

Under the supervision of

Dr. Manoj K. Sharma

Associate Professor

School of Physics and Materials Science

Thapar University, Patiala – 147004

July, 2013

I dedicate this thesis to God and my family

3

CERTIFICATE

I hereby certify that the work which has been presented in this thesis entitled, "**Study of complete fusion and incomplete fusion in the decay of $^{96}Tc^{*}$ system**" submitted for partial fulfillment of the requirements for the award of degree of **Masters of Science** in **Physics** at **Thapar University, Patiala,** is an authentic record of my own work carried out under the supervision of **Dr. Manoj K. Sharma, Associate Professor, SPMS** and refers other researcher's work which are duly listed in reference section.

The matter embodied in this thesis has not been submitted for the award of any other degree of this or any other university.

Neha Grover

Date: July 15, 2013 (Neha Grover)

This is to certify that the above statement made by the candidate is correct and true to best of my knowledge.

M Sharma
15/7/13

Dr. Manoj Kumar Sharma
Associate Professor
SPMS, Thapar University
Patiala

Countersigned by:

Dr. Kulvir Singh
(Professor & Head)
SPMS, Thapar University
Patiala

Dr. S.K. Mohapatra
Dean of academic Affairs
Thapar University,
Patiala

4

Acknowledgement

Foremost, I would like to express my sincere gratitude to **Dr. Manoj K. Sharma**, my worthy supervisor. Without him the dissertation would not have been possible. I thank him for his patience, motivation, enthusiasm, and immense knowledge. His guidance helped me in all the time of research and writing of this Dissertation. I could not have imagined having a better advisor and mentor for my Masters Degree Dissertation. I express my sincere thanks to him for his valuable guidance in caring out this work under his effective supervision, encouragement and cooperation. His visionary thoughts have influenced me greatly. His dynamical attitude has empowered me with Zeal of energy to conquer the minor details of my research work.

Besides my advisor, I also thank **Dr. Kulvir Singh, Professor & Head**, school of physics and materials science for his support and providing facilities.

My sincere thanks also goes to **Ms. Gurvinder Kaur**, research Scholar for the help and valuable suggestions provided by her. Despite having a busy schedule she was always available for discussion and guidance.

Special thanks to all my friends and the staff at the school of physics and material science for providing me a friendly atmosphere and encouraging me throughout this work.

Last but not the least; I would like to thank my family: my parents for giving birth to me at the first place and supporting me spiritually throughout my life. Their moral support has bared fruit through completion of this thesis.

Patiala

July, 2013

Neha Grover

Neha Grover

Contents

List of Figures/Tables

Abstract

With the advancement in radioactive ion beams, the study of reactions involving fusion of loosely bound nuclei form an integral part in low-energy heavy-ion physics. It is an important area of research so far as the understanding of nuclear structure, nuclear reactions and various dynamical features related to them are concerned. This is because through the study of such reactions one can infact investigate the dynamics involved in nuclei with comparatively low binding energies. These studies are of primary importance because the decay through complete fusion may not be the sole contributor towards the total cross-sections associated with the concerned reaction. Many other processes such as incomplete fusion, quasi-fission, deep inelastic collision may also be observed hence the advantage of studying such reactions is that the effect of loosely bound nucleons on fusion and subsequently on decay can be explored, which in turn provides deeper insight of various associated aspects. In this work, we have investigated the dynamics of intermediate mass $^{96}Tc^{*}$ nucleus formed in $^{6}Li+ {}^{90}Zr$ reaction in framework of Dynamical Cluster-decay Model (DCM) in reference to the recent experimental data of 2012. In order to respond to the experimental advancements, it becomes mandatory for the theoretical models to carry out the study with inclusion of extreme conditions of excitation energies, temperature, angular momentum etc. Interestingly, DCM with all these features included into it, provides information for decay patterns of nuclear system formed in heavy ion reactions. In addition to this, the study of nuclear reactions would be incomplete without the inclusion of deformation and orientation degree of freedom. The role of same is explored through DCM by carrying out the calculations for spherical and quadrupole (β_2) deformation effects. The complete fusion cross-sections for weakly bound ^{6}Li projectile with ^{90}Zr target show suppression at all energies across the barrier. This may be associated with the break-up of ^{6}Li projectile, leading to incomplete fusion. The decay study for both complete fusion and incomplete fusion processes have been carried in terms of evaporation residues (equivalently light particles) production in framework of DCM.

Chapter-I

1.1 Introduction

In order to contribute towards the area of scientific research, nuclear physics has played a crucial role since last few decades and has imparted useful information for the overall development of the world around us. These efforts have successfully provided solutions to many of the existing problems but at the same time gave birth to certain unanswered queries as well. As a result there is still a lot to be explored about and attempts for the same are being made in many fields, with study of nuclear properties being one of them. To accomplish this, a lot of new experiments have been carried out and subsequently supplemented with various suitable theoretical approaches. Also, the study of nuclear reactions and nuclear structure is of tremendous importance as it helps us to understand the behavior of a nucleus, its formation and decay to a greater extent. With the advancement in experimental field, the theoretical study of nuclear reactions, nuclear structure and related dynamics demands the involvement of various extremities like temperature, angular momentum and excitation energy etc.

In low energy regime, the study of heavy ion reactions provides an opportunity to investigate the interaction between the ions involved and behavior of the potentials governing them. It also helps us to analyze the extent of stability of a nucleus, various decay mechanisms involved and estimation of the cross-sections. In addition to these informative features, study of heavy ion reactions also contributes towards the synthesis of new elements. Moreover, the analysis of fusion of heavy-ions at low energy has been found to be of much interest in recent times with the advent of radioactive ion beams. Heavy ion reactions can be categorized on many grounds. However, on the basis of nuclei involved in a reaction or more precisely based on the behavior of projectile and its interaction with the target nucleus, the reactions may be categorized as complete fusion reactions and direct reactions.

1.2 Fusion Reactions

In 1936, Neil Bohr gave a very interesting concept of intermediate state i.e. compound nucleus, which forms an important part for the study of nuclear reactions. In a nuclear reaction, fusion is an amalgamation of two interacting nuclei to form a highly excited, equilibrated compound nucleus, which decays by successive particle emission to produce evaporation residues and/or undergoes fission. The residual nucleus, from which further particle emission is energetically not possible, decays to the ground state by emitting γ-ray cascades.

The fusion cross-sections are determined by summing the cross-sections of the evaporation residues and adding them to the fission cross-sections, if any. In general, the decay of compound nucleus does not depend on the process of its formation and hence may decay through any mechanism. Although in certain cases entrance channels are seen to influence the decay processes. Therefore a proper analysis of entrance channel effects is of extreme interest in reference to overall understanding of nuclear dynamics associated with a nuclear reaction.

On the basis of mass of compound nucleus formed there may be different dominant decay modes. For light compound systems with A_{CN} ~ 40-80, the light-particles (LPs, $0 < Z < 2$ and $A \leq 4$) emission is always accompanied by intermediate mass fragments, the IMFs (with $2 < Z < 10$ and $5<A<20$). In general the IMFs contribution is very small of the order of 5-10%, in comparison to LPs contribution. However, for the heavy nuclear systems A_{CN} >> 200, the most probable decay mode of the compound nucleus is fission/ heavy mass fragments (HMFs) ($20<A<A/2$), due to its instability against centrifugal repulsion, with small contribution from neutrons and γ-rays emissions, just in contrast to decay process of light compound systems. For intermediate nuclear systems having mass A_{CN} ~ 80-200, there is competition between light particles and fission processes.

However, in the reactions where at least one of the colliding nuclei is loosely bound, breakup may become an important process and hence influence the flux going into fusion. Interest in the investigation of the effect of breakup on fusion at energies around the coulomb barrier has received a fllip in recent years, primarily owing to the recent availability of radioactive ion beams in different laboratories around the world. It is known that some of these nuclei away from the β-stability line are characterized by halo/skin structure and large breakup probabilities are associated with them. A detailed understanding of the fusion mechanism with loosely bound nuclei is very significant for understanding of nuclear reactions and for the production of new nuclei near the drip lines.

1.3 Direct reactions

Direct reactions are those reactions in which nuclei make glancing contact and then separate rapidly. Projectile may exchange some energy and / or angular momentum, or have one or more nucleons transferred to it or removed from it, and mostly take place at or near the nuclear surface and at larger impact parameters. In these reactions projectile reacts with only one, or a few, nucleons of the target [1]. Because of the reduced compound formation probability these reactions are equally important for study of nuclear dynamics. Light-ion induced fusion evaporation or direct reactions produce a limited number of neutron-deficient species and rare isotopes close to stability at high conversion rates [2].

1.4 Loosely Bound Nuclei

In 1985, when it was being felt that nuclear physics has possibly reached at its saturation, a drastic change in scenario occurred with the discovery of a loosely bound isotope of lithium. The internal structure of such loosely bound nuclei is found to deviate from the conventional spherical shell structure, a known characteristic of nuclei close to the line of stability. Reactions induced by weakly bound nuclei have a number of specific features.

Processes of cluster transfer and the breakup of the bombarding nucleus with the subsequent capture of the residue nucleus by the target nucleus (breakup or breakup fusion) play an important role in these reactions. In loosely bound nuclei where break-up is important, energies around 7 MeV/nucleon are known to lead to sizable effects on the dynamics of a reaction [3]. With a pronounced cluster structure and low Z, ^{6,7}Li projectiles are fragile, and can therefore, exhibit a range of phenomena, mostly of a nuclear nature and therefore can also be used for the study of elastic scattering of stable loosely bound nuclei with similar masses [4]. Also, transfer reactions involving relatively light, loosely bound nuclei are used in nuclear astrophysics. In reactions involving such nuclei, grazing angle plays a crucial role as it becomes much easier to identify the sequential breakup observed due to projectile breakup if the measurement is done beyond the grazing angle. Also it has been observed that the direct breakup part dies out with the increase of scattering angle where the sequential contributions remain significant [5].

1.5 Fusion of Loosely Bound Systems

For fusion to occur, the system must overcome the barrier resulting from the sum of the repulsive Coulomb potential and the attractive nuclear potential. Fusion reactions with weakly bound projectiles are interesting because of their importance in astrophysical reactions, in understanding the nucleosynthesis process and in studying nuclei near the drip lines. For example loosely bound ^{6}Li may interact with deuteron to form two α-particles via an intermediate compound system ^{8}Be.

$$^{6}\text{Li} + {}^{2}\text{H} \rightarrow {}^{8}\text{Be} \rightarrow {}^{4}\text{He} + {}^{4}\text{He}$$

Such loosely bound interactions exhibit properties such as low breakup threshold due to low binding energy per nucleon and thus have very few unbound excited states, larger rms radii compared to the value obtained from systematics ($R = roA^{1/3}$), larger transfer probability etc. Owing to this anomalous behavior, the reactions induced by weakly bound nuclei possess a number of specific features. Recent experimental studies of these processes have been developing rather intensely due to the application of beams of radioactive nuclei and beams of accelerated stable weakly bound nuclei such as ^{6}Li, ^{7}Li,

^{9}Be, the two-neutron halo nucleus ^{6}He, the one-neutron halo nucleus ^{11}Be, and the one-proton halo nucleus ^{8}B on light, medium and heavy targets.

It has been realized recently that for intermediate and heavy nuclei the direct mechanism can become important near the shell closures and for neutron rich isotopes where the level density becomes too low for the CN mechanism [6]. In the case of fusion of the stable weakly bound projectiles with intermediate and heavy mass targets, a general observation of suppression of the CF cross sections has been reported at above-barrier energies. Suppression (or enhancement) observed in reaction involving loosely bound nuclei may be considered, as a consequence of fusion near the barrier, which is strongly affected by intrinsic degrees of freedom of the interacting nuclei, and effectively causes a splitting in energy of the fusion barrier. This gives rise to a distribution of barrier heights and is manifested most obviously as suppression or (enhancement) of the fusion cross sections at energies near the barrier. Generally with loosely bound projectiles, breakup may result in capture of only a part of the projectile, thus suppressing complete fusion [7].

Apart from dealing with suppression, certain other difficulties also need to be accounted in the study of complete-fusion (CF) reactions using weakly bound projectiles due to breakup process involved. The Evaporation residues subsequent to CF are very similar to, or even coincident with, those coming from incomplete fusion (ICF), i.e., reactions in which one of the break-up fragments of the projectile fuses with the target. Therefore, what is usually obtained is the total fusion cross section, that is, the sum of CF and ICF cross sections. At both experimental and theoretical grounds, efforts have been done to measure the individual contribution of complete fusion and the competing incomplete fusion (ICF) processes. It needs to be pointed out that to carry out a meaningful study of the influence of breakup on fusion, one need to disentangle the CF and ICF events and measure their cross-sections.

1.6 Breakup cross-sections

In the case of reactions where loosely bound projectiles are involved, breakup becomes one of the important reaction channels. It has been known for some time that a significant fraction of the total cross section arises from the breakup of the incident nucleus and has been studied several times at various bombarding energies above, around, and below the Coulomb barrier. Only Coulomb effects, however, should contribute to the breakup at incident energies below the Coulomb barrier [8]. It has been observed that breakup may suppress the possibility of fusion owing to only partial fusion of some of the projectile fragments [9]. Breakup can be of two types: exclusive breakup, with two fragments in the exit channel and the target in its ground state, and inclusive breakup, with at least one outgoing α particle. The ratio of these two absolute cross-sections needs to be fully investigated. The inclusive breakup is much larger than the exclusive process. By the name ‘‘inclusive breakup’’ adopted for the strong reaction channels, we indicate all the events that show at least one outgoing α-particle, regardless of their origin that might be ‘‘pure breakup’’ or a more complex reaction mechanism. The breakup process is mainly sequential, i.e., the projectile excitation, and the consequent breakup, occurs along a Coulomb-like trajectory of the center of mass (c.m.) of the fragments. The study of the breakup of light-ion projectiles like ^{6}Li is of special interest since its cluster nature simplifies calculations which can corroborate experimental results and therefore enlighten this subject. ^{6}Li is a weakly bound nucleus ($^{6}\mathrm{Li} \rightarrow \alpha + \mathrm{d}$), which resembles the halo nucleus ^{6}He. In this context, a study of its direct and sequential breakup may help in understanding the breakup process in halo nuclei. The breakup fragments α and deuteron ^{2}H, may originate either by a sequential or/and a direct process. In all simulations, the breakup fragments are assumed to be emitted isotropically in the rest frame of ^{6}Li.

Heavy-ion induced reactions at energies below 10 MeV/A have in common the fact that the reaction cross section is shared predominantly among complete fusion and one of the following competing processes: those leading to incomplete fusion (ICF), deep-inelastic collisions, and quasi fission (QF) [10].

1.7 Incomplete Fusion

Complete fusion (CF) is defined as the sum of direct complete fusion (DCF) and sequential complete fusion (SCF). Where in DCF, whole of the projectile fuses with whole of the target and in SCF, the projectile breaks up and subsequently all the fragments fuse with the target to form a compound nucleus similar to that in the DCF process Hence CF process is defined as the capture of entire projectile by target nucleus [11]. The Compound Nucleus (CN) formed via CF is expected to have pre-determined mass/charge, excitation energy and angular-momenta [12] and the entire angular momentum of the projectile is transferred to the composite nucleus [13].

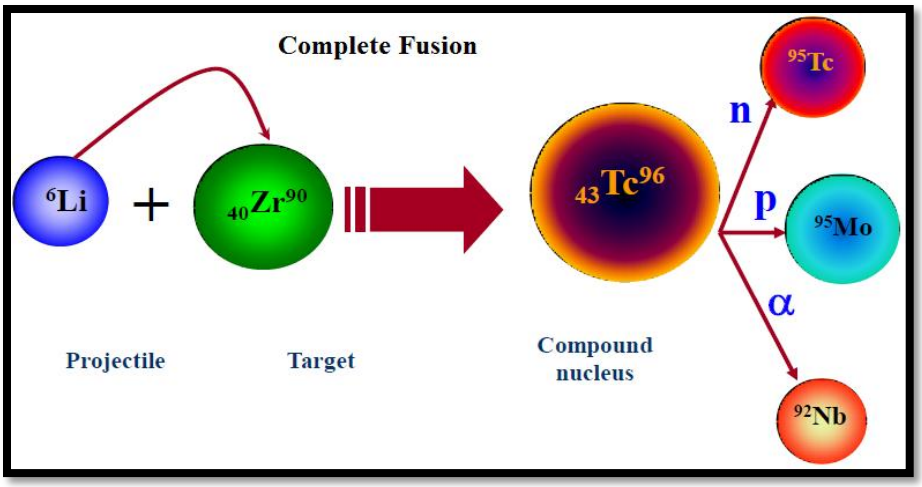

Fig.1.1 *Schematic diagram for Complete Fusion of ^{6}Li projectile with ^{90}Zr target*

In ICF processes, the projectile is speculated to break up into α cluster as it approaches the nuclear force field of the target nucleus. In the second part of this binary process, one of the fragments of the projectile is assumed to amalgamate with the target nucleus to form an incompletely fused composite system and the remaining fragment is considered to move nearly undeviated in the forward cone with almost projectile velocity [14]. The momentum transfer is essentially proportional to the mass of the fusing fragment in ICF [15]. Incomplete-fusion reactions appear to be a natural extension of the fusion process for those collisions for which angular momentum limitations do not allow complete

fusion. Specifically for loosely bound nuclei, projectile fragmentation sets in rapidly at the cost of the decreasing cross section for fusion and incomplete-fusion reactions. In recent years, the competition between incomplete fusion (ICF) and complete fusion (CF) reaction dynamics at energies in the vicinity of Coulomb barrier (CB) has been a topic of extensive discussion among experimental as well as theoretical nuclear physicists The ICF reactions were observed around five decade ago by Britt and Quinton in the bombardment of ^{197}Au and ^{209}Bi by ^{12}C, ^{14}N, and ^{16}O projectiles at energies ≈10.5 MeV/nucleon [14]. Generally CF is assumed to be the sole contributor to the total fusion cross section at near barrier energies. However, in several studies a significant fraction of ICF has also been observed at these energies.

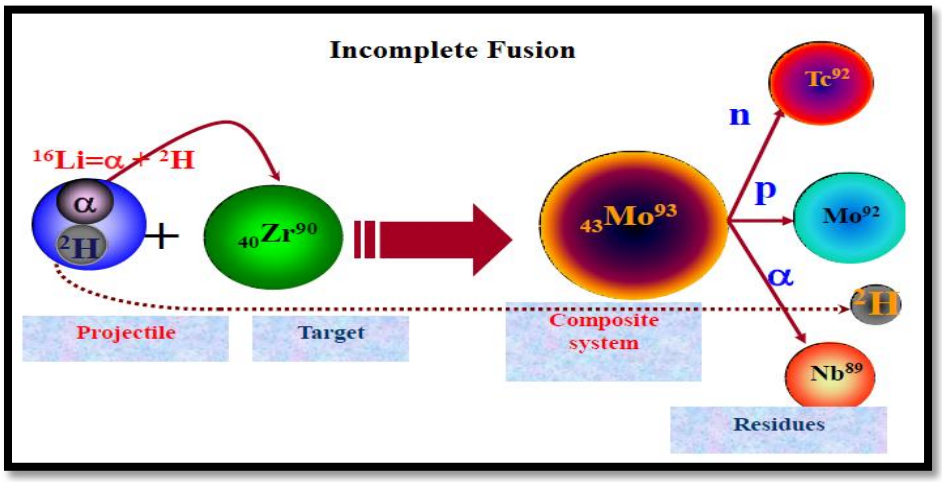

Fig.1.2 *Schematic diagram for Incomplete Fusion (ICF) of loosely bound* $^{6}Li \rightarrow \alpha + {}^{2}H$ *with* $^{90}_{40}Zr$ *target*

In recent years there has been growing experimental interest in the ICF reactions for studying neutron rich nuclei, which cannot be reached by CF process [16]. Usually the residues following both (CF and ICF) processes are very similar or identical, and therefore the charged particle detectors are not able to distinguish them. This is even more dramatic for light systems for which the main evaporation channels include charged particles (protons and alphas). Therefore, most of the data available in the literature correspond to total fusion (TF) cross section. Even when this separation is possible, one

cannot distinguish between CF and fusion of all the charged break-up fragments with the target. Hence, it is very difficult to distinguish experimentally the ICF from direct transfer channels leading to the same compound nucleus [17]. However some efforts have been made and some data is made available in reference to ICF process.

1.8 Deep inelastic collision

In nuclear physics, the compound nucleus formation reactions have been successfully used as it is a common mode of reaction. A significant study of reactions involving non-compound nucleus is also important. Along with the incomplete fusion process another process involving non-compound nucleus formation is deep inelastic collision (DIC) in which there is exchange of nucleons between the target and the projectile nuclei. As a result of this a considerable amount of kinetic energy is dissipated. Generally, projectile like fragments (PLF) are obtained as decay products in DIC .When the projectiles are low energy nucleon or alpha particles, approximately head on collisions of heavy ions at low energy is also liable to produce a compound nucleus but when the impact parameter lies between the grazing and head on limits then the interaction between low energy heavy ions is likely to result in a deep inelastic collision. In this process projectile may loose most of its energy as it enters in to the target nuclei. Also we can produce the neutron rich nuclei by means of Deep inelastic collision (DIC). Although the mass distribution is broad, it is possible that we can have a wide choice of the target and projectile combination for the DIC processes. Deep inelastic collision occurs in heavy ion reactions at projectile energies 5-10Mev/nucleon [18]. The angular momentum dissipation in deep inelastic collisions has been estimated from the data and it has been found to be close to the corresponding sticking limit value [19].

1.9 Quasi fission

In Quasi-fission (QF) process, the compound nucleus is not formed to the full that is the mass degree of freedom is out of complete equilibrium [20]. Quasi fission is a dynamical non-equilibrium process. It results when the combined system formed after capture breaks apart into two fragments before a compact compound nucleus is formed. The probability of quasifission and the characteristics of the quasifission products are understood to depend on the diffusive motion over the multi-dimensional potential energy surface. This motion results either in a compact shape (fusion) or in an elongating dinuclear shape leading to quasifission. Partly because quasifission characteristics can depend in a complex way on many variables and partly from the overlap of quasifission and fusion-fission events generally found in experiments, quasifission is still not fully understood. As a wholly dynamical process, a key quantity characterizing quasifission is its timescale that is the "sticking time" between capture and breakup (scission). Measurements of quasifission mass-angle distributions (MAD) at GSI in the 1980s showed that timescale to be typically shorter than the rotation time equivalent to 10^{-20}s. This is significantly shorter than the typical timescale of fusion fission [21].

In heavy ion-induced reactions the CN formation cross section is suppressed strongly by competing quasifission process (QF). Therefore, the measurement of binary reaction channel gives the information about the competition between fusion-fission and QF processes and allows estimating the probability of the CN formation [22].

1.10 Importance of ^{6}Li+ ^{90}Zr $\rightarrow$ ^{96}Tc* reaction

In this work we have carried out the study to find complete fusion cross-sections having contribution of light particles or equivalently evaporation residues in the intermediate mass nucleus ^{96}Tc* formed in ^{6}Li+^{90}Zr reaction in framework of Dynamical Cluster-decay Model (DCM). Also, incomplete fusion cross-sections observed due to break-up of ^{6}Li projectile into α+d channel are explored. There are many interesting features in this

reaction that motivated us to study it in detail. With the presence of ^{6}Li projectile, the effect of break-up on the fusion and decay of intermediate mass nucleus is of interest. Also the target ^{90}Zr is neutron magic nucleus (N=50) so it is expected to play an important role in the dynamics of chosen reaction. Moreover, the neutron rich ^{96}Tc* is quadrupole deformed and hence the role of deformations in its decay would be worth studying.

As the role of excitation energy (or temperature), deformation and orientation of decaying fragment is of extreme importance in context to dynamical features of nuclear reactions, the same are addressed in this work. The magnitudes of both the quadrupole (β_2) and the hexadecapole (β_4) deformations of the reaction partners play an important role in formation and decay of a compound nucleus. The deformations and orientations of nuclei change both the position and depth of the nuclear potential. It has been observed that majority of deformed nuclei have an elongated, cigar-like prolate shape, while there are only few flattened, oblate nuclei. This has attracted the attention of nuclear physicists for more than half a century. A definitive explanation for the origin of this is still a matter of discussion and represents a fundamental challenge in nuclear structure physics. The sign of the quadrupole deformation parameter β_2, extracted from measured electric quadrupole moments, determines the nuclear shape: $\beta_2 > 0$ corresponds to prolate, $\beta_2 = 0$ to spherical, and $\beta_2 < 0$ to oblate deformation. To describe the ground state deformations, shell effects must be taken into account. It is relevant to mention here that the pure quadrupole deformed nuclei and the nuclei with normal (large or small) quadrupole deformation plus small-positive or negative hexadecapole deformation result in an ec (equatorial compact) configuration. On the other hand the ones with normal (large or small) quadrupole deformation plus large-positive hexadecapole deformation gives rise to an nec (non-equatorial compact) configuration [23]. However in present work we have confined ourselves to quadrupole deformations only.

References

[1] C. Giusti, A. Meucci et al. J. Phys.: Conference Series **366,** 012019, (2012).

[2] C.A. Bertulani, A. Gade Physics Reports **485**, 195-259, (2010).

[3] L. Trache, A. Azhari, H. L. Clark, et al. Phys. Rev. C **61**, 024612, (2000).

[4] F. Carstoiu, L. Trache, Robert E. Tribble, Phys. Rev. C **70**, 054610, (2004).

[5] Chhanda samanta, J. Phys., **Vol.** 57, 2, Aug, (2001).

[6] T. Rauscher, R. Bieber and H. Oberhummer et al. Phy. Rev. C, **57**, 4,(1998).

[7] M. Dasgupta, D. J. Hinde, J. O. Newton et al., Phys. Rev. Lett. **82**, 7, (1999)

[8] R. Ost, E. Speth, K. O. Pfeiffer and K. Bethge, Phys. Rev. C **5**, 6, (1972).

[9] H. Kumawat, V. Jha, V. V. Parkar, et al. Phys. Rev. C **81**, 054601, (2010).

[10] H. Morgenstern, W. Bohne, W. Galster et al. Phys. Rev. Lett. **52**, 13, (1984).

[11] A Mukherjee and M.K Pradhan, Pramana J. Phys., **Vol.** 75, 1, (2010).

[12] P.P. Singh, A. Yadav et al. Journal of Physics: Conference Series **282,** 012019, (2011).

[13] S. Gupta, B. P. Singh et al. Phys. Rev. C **61**, 064613, (2000).

[14] K. Kumar, T. Ahmad, et al. Phys. Rev. C **87**, 044608, (2013).

[15] D. J. Parker, j.Asher, T. W. Conlon, I. Naqib et al. Phys. Rev. C **30**,1, (1984).

[16] D. Singh, R. Ali, M. Afzal Ansari et al. Nuclear Physics A **879**, 107, (2012).

[17] P.R.S. Gomes, M.D. Rodríguez et al. Physics Letters B **601**, 20, (2004).

[18] T. Ishii, M. Itohb, M. Ishii", A. Makishima", M. Ogawab, I. Hossainb, T. Hayakawaa, T. Kohnob, Nuclear Instruments and Methods in Physics Research A **395**, 210, (1997).

[19] S. Kundu, C. Bhattacharya, K. Banerjee et al. Phys. Rev. C **85**, 064607, (2012)

[20] C. J. Lin, H. Q. Zhang, K. Nishio, H. Ikezoe et al. Journal of Physics: Conference Series **420**, 012126, (2013).

[21] D J Hinde, M Dasgupta et al. Journal of Physics: Conference Series **420**, 012115, (2013).

[22] M Itkis, Journal of Physics: Conference Series **413,** 012003, (2013).

[23] R. K. Gupta, M. Manhas and W. Greiner, Phys. Rev. C **73**, 054307, (2006).

Chapter-II

The Dynamical Cluster Decay Model (DCM)

The Dynamical Cluster-Decay Model [1-6] (DCM) is an adaptation of the preformed cluster model (PCM) of Gupta et al. or we can say that it is extension form of (PCM) [7, 8] which is for ground state decays, and is based on the well-known Quantum Mechanical Fragmentation Theory, QMFT [9-12].

Introduction to DCM

DCM (dynamical cluster model) has been established for the study of heavy ion reaction dynamics especially for the decay of excited compound nucleus. The deformations and orientations effects of reaction partners and decay products are explicitly included in this model along with temperature and angular momentum contributions. It has been used to study the decay of various compound nucleus lying in different mass regions e.g. light mass elements ($^{48}Cr^{*}$, $^{56}Ni^{*}$), intermediate mass ($^{116,118,122}Ba^{*}$, $^{164}Yb^{*}$), heavy ($^{176\text{-}196}Pt^{*}$, $^{201}Bi^{*}$, $^{202}Pb^{*}$, $^{204}Po^{*}$, $^{217}Fr^{*}$, $^{219,220}Ra^{*}$, $^{246}Bk^{*}$) and super-heavy ($^{286}112^{*}$, $^{286}114^{*}$, $^{297}117^{*}$) region.

This model is worked out in terms of only one parameter fitting, the neck-length parameter ΔR. The emission of the light particles (LP), with $A_2 \leq 4$, $Z_2 \leq 2$, as well as the complex intermediate mass fragments (IMF), $5 < A_2 < 20$, $2 < Z_2 < 4$, along with possible fission fragments is considered as the dynamical collective mass motion of preformed clusters through the barrier. DCM model is worked out in terms of the collective coordinates of mass and charge asymmetries $\eta = A_1 - A_2/A_1 + A_2$ and $\eta_Z = Z_1 - Z_2/Z_1 + Z_2$, relative separation R, deformations and orientations.

For η-motion and to find the preformation probability P_0, we solve the stationary Schrödinger equation in the form of η**,** at a fixed relative separation $R=R_a$, and that schrodinger equation is given as follow:-

$$\left\{-\frac{\hbar^2}{2\sqrt{B_{\eta\eta}}}\frac{\partial}{\partial\eta}\frac{1}{\sqrt{B_{\eta\eta}}}\frac{\partial}{\partial\eta}+V_R(\eta,T)\right\}\psi^{\nu}(\eta)=E^{\nu}\psi^{\nu}(\eta) \qquad (1)$$

With $\nu = 0, 1, 2, 3\ldots$where ($\nu = 0$) refers to ground state and other greater values refer to the excited state solutions.

$B_{\eta\eta}(\eta)$ is smooth classical hydro dynamical masses [13] and represents the kinetic energy part in Eq.(1).

The solutions of Eq. (1) give the preformation probability as follow:

$$P_0 = \sqrt{B_{\eta\eta}}\ |\ \Psi[\eta(A_i)]\ |^2\ (\frac{2}{A}) \qquad (2)$$

Where (i=1 or 2) and Ψ(η) is $\Psi^{\nu=0}(\eta)$ if the ground-state solution is chosen.

Now in incomplete fusion (ICF) processes only a part of the projectile interacts with the target, so we can calculate P_0 in same way as that of the compound nucleus (CN) process with only one difference that in case of ICF composite system will be different depending upon the breakup of the projectile.

The temperature T (in MeV) is related with excitation energy of compound nucleus (CN) as follow:

$$E^*_{CN} = \left(\frac{A}{9}\right)T^2 - T \qquad (3)$$

Now to calculate the energy of ICF projectile, let A^T represents the total mass number of projectile before break-up, then the energy of the projectile would be:

$$E_{Projectile} = \frac{E}{A} * A^T \quad (4)$$

Further if A^F is the mass number of the fragment which does not hit the target but moves in straight direction with the same velocity as that of the projectile so energy of this fragment can be find by the following expression:

$$E_{fragment} = \frac{E}{A} * A^F \quad (5)$$

Now we can find the energy of projectile after breakup with the help of Eq. (4) and Eq. (5) and the expression for energy of projectile in ICF processes is given by [6]:

$$E_{ICF}^{P} = \frac{E}{A} * A^T - \frac{E}{A} * A^F \quad (6)$$

The CF and ICF events can be disentangled on the basis of the degree of linear momentum transfer (LMT) from the projectile to the target nucleus. In the case of CF, entire nucleonic degrees of freedom of projectile and target nucleus blend to form an equilibrated compound nucleus (CN) with predetermined physical properties, e.g. charge, mass, recoil velocity, etc. However, the ICF events originate from the fractional LMT followed by projectile breakup. The ℓ values from $\ell = 0$ to ℓ_{crit} lead to the CF events; however, for $\ell \geq \ell_{crit}$, ICF events are expected to set in. In the latter case, (for ℓ values higher than ℓ_{crit}) the absence of potential pocket forbids fusion until a part of the projectile is released to provide sustainable input angular momenta [14].

Penetrability (P) that refers to R-motion is calculated as the WKB tunneling probability solved analytically in Ref. [7, 8] and is given by:

$$P = \exp\left[-\frac{2}{\hbar}\int_{R_a}^{R_b}\{2\mu[V(R)-Q_{eff}]\}^{1/2}dR\right] \quad (7)$$

The first tunneling point R_a is defined as $R_a = R_t(\eta) + \Delta R = R_t(\alpha, T) + \Delta R(T)$

The radius vector $R_i(\alpha,T)$ is given by :

$$R_i(\alpha_i, T) = R_{0i}(T)\left[1 + \sum_{\lambda} \beta_{\lambda i} Y_{\lambda}^{(0)}(\alpha_i)\right] \quad (8)$$

Where $R_{0i}(T)$ is given by [15]:

$$R_{0i} = [1.28A_i^{1/3} - 0.76 + 0.8A_i^{-1/3}](1 + 0.0007T^2) \quad (9)$$

This value of R (instead of the compound nucleus radius R_0) assimilates to a good extent the effects of both, deformations β_i of two fragments and neck formation between them [16].

Now by having the value of preformation probability (P_0) from Eq. (2) and penetrability (P) from Eq. (7) both depending on angular momentum (ℓ) and temperature (T), we can calculate the decay cross-section in terms of partial wave with the help of DCM as follows:-

$$\sigma = \frac{\pi}{k^2} \sum_{\ell=0}^{\ell_{max}} (2\ell + 1) P_0 P \quad (10)$$

Where value of k is given by: - $k = \sqrt{\frac{2\mu E_{c.m}}{\hbar^2}}$

The reduced mass:-

$$\mu = \left[\frac{A_1 A_2}{(A_1 + A_2)}\right] m = \frac{1}{4} Am(1 - \eta^2)$$

Where m is the nucleon mass and ℓ_{max} is the maximum angular momentum which is fixed for the vanishing of the fusion barrier of the incoming channel η_i or the light particle cross-section $\sigma_{LP} \rightarrow \mathbf{0}$.

The Q_{eff} can be expressed in terms of binding energies as follows:

$$Q_{eff}(T) = B(T) - [B_1(T=0) + B_2(T=0)] = TKE(T) = V(R_a) \tag{11}$$

The deformation and orientation dependent fragmentation potential that forms an input in Eq. (1) is given as:

$$V_R(\eta, T) = \sum_{i=1}^{2}[V_{LDM}(A_i, Z_i, T)] + \sum_{i=1}^{2}[\delta U_i]\exp(-T^2/T_0^2) + V_c(R, Z_i, \beta_{\lambda i}, \theta_i, T) \tag{12}$$
$$+ V_P(R, A_i, \beta_{\lambda i}, \theta_i, T) + V_\ell(R, A_i, \beta_{\lambda i}, \theta_i, T)$$

Where the T-dependent liquid drop energy $V_{LDM}(T)$ is that of [17], with (Seeger's) constants at $T = 0$ refitted to give binding energies of [18], defined as $B = V_{LDM}(T=0) + \delta U$ The shell corrections are calculated in the "empirical method'' of Myers and Swiatecki [19].

The V_P is the nuclear proximity potential, which is also considered temperature dependent here and is given by,

$$V_p\left(S_0(T)\right) = 4\pi\,\bar{\mathrm{R}}(\mathrm{T})\gamma\mathrm{b}(\mathrm{T})\varphi(\mathrm{S}_0,(\mathrm{T})) \tag{13}$$

Where $\bar{R}(T)$ and $\phi(s_o, T)$ in Eq. (13) are, respectively, the inverse of the root mean square radius of the Gaussian curvature and the universal function, which is independent of the geometry of the system.

V_C is coulomb potential which is also temperature dependent. The coulomb potential for co-planar (φ =0) and deformed nuclei, is given by:

$$V_C = \frac{Z_1 Z_2 e^2}{R} + 3Z_1 Z_2 e^2 \sum_{\lambda,i=1.2} \frac{1}{2\lambda+1} \frac{R_i^{\lambda}(\alpha_i)}{R^{\lambda+1}} \mathrm{Y}_{\lambda}^{(0)}(\theta_i) \left[\beta_{\lambda i} + \frac{4}{7}\beta_{\lambda_i}^2 \mathrm{Y}_{\lambda}^{(0)}(\theta_i)\right] \quad (14)$$

Where Z_i (i=1, 2) are the atomic no's, $\beta_{\lambda i}$ are deformations with λ=2, 3, 4…., and R is radius. The orientation angles are represented through α and θ.

References

[1] M. K. Sharma, G. Sawhney, R. K. Gupta, and W. Greiner, J.Phys. G: Nucl. Part . Phys. **38**, 105101, (2011); M. K. Sharma, G. Sawhney, S. Kanwar, and R. K. Gupta, Mod. Phys. Lett. A **25**, 2022, (2010).

[2] M. Kaur, R. Kumar, and M. K. Sharma, and M. K. Sharma, Phys. Rev. C **85**, 014609, (2012).

[3] M. Balasubramaniam, R. Kumar, R. K. Gupta, C. Beck, and W. Scheid, J. Phys. G: Nucl. Part. Phys. **29**, 2703, (2003).

[4] B. B Singh, M K Sharma and R K Gupta, Phys. Rev. C **77**, 054613, (2008).

[5] M. Kaur, Manoj K. Sharma, And Raj K. Gupta, Phys. Rev. C **86**, 064610, (2012).

[6] G. Kaur and M. K. Sharma, Nucl. Phys. A **884**, 36, (2012); G.kaur and M.K. Sharma, Phys. Rev. C 87,044601, (2013).

[7] D.N Poenaru and W Greiner J. Phys. G: Nucl. Part. Phys. **17,** S443, (1991).

[8] S.S Malik and R. K. Gupta, Phys. Rev. C **39**, 1992, (1989).

[9] J. Maruhn and W. Greiner, Z. Phys. **251,** 431, (1972).

[10] J. Maruhn and W. Greiner, Phys. Rev. Lett. **32**, 548, (1974).

[11] R.K Gupta, W. Scheid, and W. Greiner, Phys. Rev. Lett. **35**, 353, (1975).

[12] R.K. Gupta and W. Greiner, Heavy Elements and Related New Phenomena, World Scientific, Singapore, edited by W. Greiner and R.K Gupta, **Vol**. I, 397, (1999).

[13] H. Kroeger and W. Scheid, J. Phys. G: Nucl. Phys. **6**, L85, (1980).

[**14**] A Yadav, V R. Sharma, Pushpendra P. Singh et al. Phys. Rev. C **86**, 014603, (2012).

[15] G. Royer and J. Migner, J. Phy. G **18**, 1781, (1992).

[16] C. Karthikraj, N. S. Rajeswari, and M. Balasubramaniam Phys. Rev. C **86**, 014613 (2012).

[**17**] N.J. Davidson, S.S. Hsiao, J. Markram, H.G. Miller, and Y. Tsang, Nucl. Phys. A **570**, 61C, (1994).

[**18**] G. Audi and A.H. Wapstra, Nucl. Phys. A **595**, 4, (1995).

[**19**] W. Myers and W.J. Swiatecki, Nucl. Phys. A **81**, 1, (1966).

Chapter-III

3.1 Introduction

The study of reactions induced by loosely bound projectiles help us to understand the behavior of exotic nuclei and their influence on nuclear reactions. Also they are of great importance for synthesis of new elements. Hence, with an aim to study the nuclear structure and reaction dynamics for loosely bound nuclei an attempt has been made to study the decay processes involved in fusion of ^{6}Li projectile with spherical neutron magic ^{90}Zr target (N=50). In reference to the available experimental data [1], the decay study for intermediate mass nucleus ^{96}Tc* formed in ^{6}Li + ^{90}Zr reaction has been done in framework of dynamical cluster-decay model (DCM) [2-9]. The calculations have been carried out at all energies across the Coulomb barrier. Interestingly, at all the energies the evaporation residues ($A_2 \leq 4$) form the most contributing decay process. It is worth mentioning that with the involvement of loosely bound ^{6}Li projectile, suppression at all energies across barrier of the complete fusion cross-sections is observed. This suppression may be associated with the fact that with loosely bound projectile there arises the possibility of having contribution from incomplete fusion (ICF) process along with that of complete fusion process. Hence, in DCM calculations the contribution of both complete fusion and incomplete fusion processes is observed. It is worth mentioning that the calculations have been done using only parameter of DCM, the neck-length parameter ΔR. Also, the role of deformation in the decay of ^{96}Tc* has been observed by taking into account the spherical and quadrupole (β_2) deformed fragmentation approaches. The calculations have been done using level density a = 9. In this chapter, the details for the behavior of fragmentation potential and corresponding preformation probabilities have been discussed. It must be noted that in DCM based calculations the minimum in the fragmentation potential corresponds to maximum in preformation probability which eventually results into higher magnitude of cross-sections for that decaying fragment.

To observe the decay mechanism of $^{96}Tc^{*}$ system across the Coulomb barrier, the variation of fragmentation potential as a function of light fragment mass A_2 is plotted as shown in Fig.3.1 for spherical choice of fragmentation. Interestingly, except for change in magnitude, there is no significant change in the structure of the fragmentation potential at two extreme energies across the barrier (refer fig 3.1 (a) for below barrier fragmentation and fig 3.1 (b) for above barrier case). The neck-length parameter ΔR, increases with increases in energy and changes considerably from 0.780 fm at $E_{c.m.}$=13.9 MeV to 1.526 fm at $E_{c.m.}$=28.0 MeV. The cross-sections have been summed up to $\ell = \ell_{max,}$ where ℓ_{max} is decided at a point for which the evaporation residue cross-sections turn to be negligibly small, $\sigma_{ER} \rightarrow 0$. For spherical choice of fragmentation, the ℓ_{max} remains same at both extreme energies being $\ell_{max} = 66\hbar$.

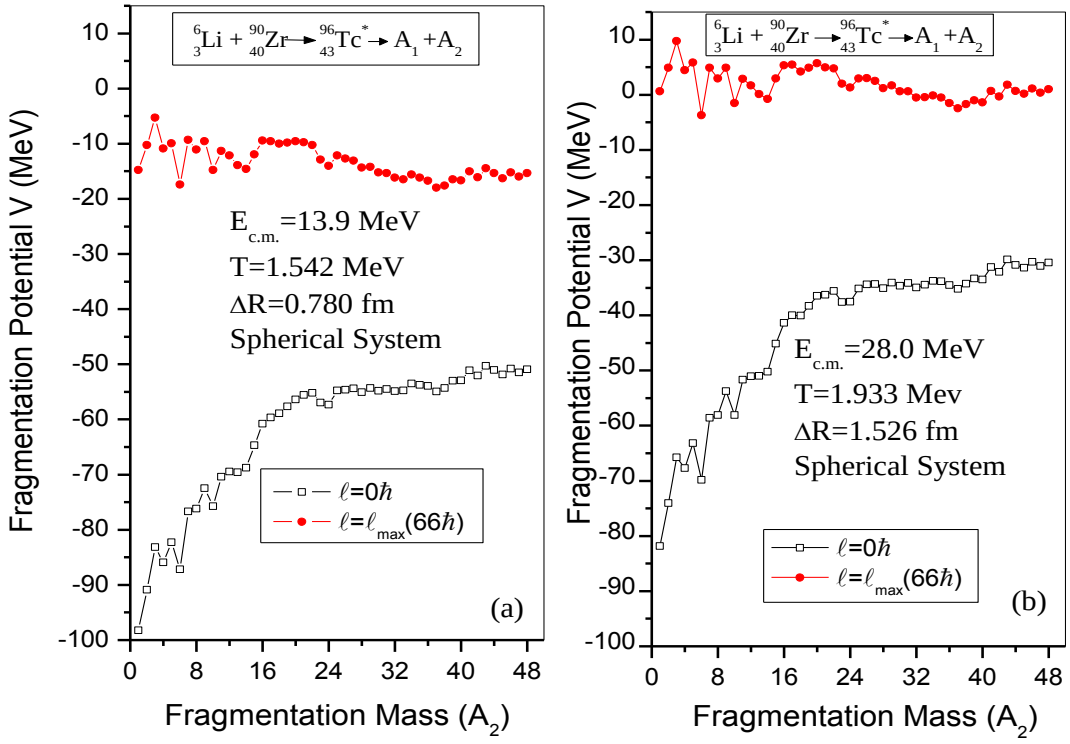

Fig. 3.1 *Fragmentation potential as a function of fragment mass (A_2) for spherical fragmentation at (a) $E_{c.m.}$ =13.9 MeV and (b) $E_{c.m}$=28.0 MeV.*

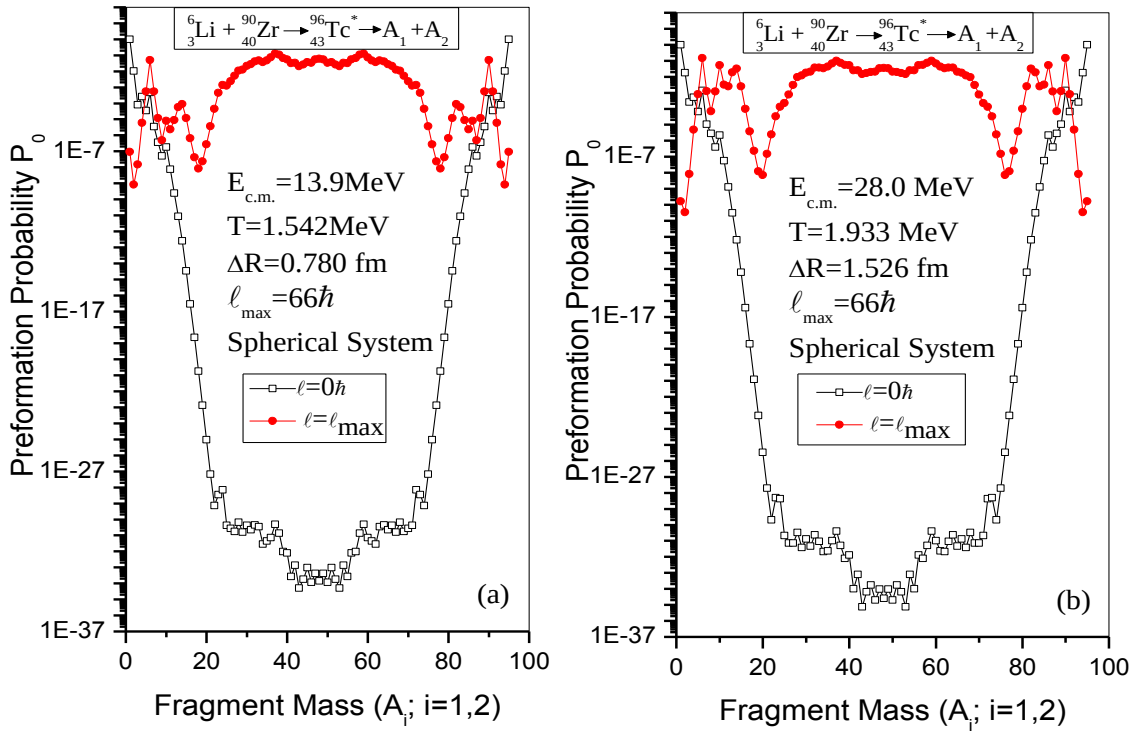

Fig.3.2 *Preformation probability as a function of fragment mass for spherical fragmentation at (a) $E_{c.m.}$ =13.9 MeV and (b) $E_{c.m.}$ =28.0 MeV.*

Fig. 3.2 shows the preformation probability as a function of fragment mass A_i (i=1, 2) at ℓ=0ħ and ℓ= ℓ_{max} for extreme energies across the barrier using spherical fragmentation. At lower ℓ-value the contribution of evaporation residue is maximum and that of fission fragment is negligibly small. However, with increase in the angular momentum the relative contribution changes as a result of which the fission fragment start competing with evaporation residues at higher ℓ-values. Also with change in energy, the magnitude of preformation probability (P_0) changes. Comparing Fig. 3.2 (a) and (b) it has been observed that few intermediate mass fragments, IMFs lying in range of A_2=9-14 are suppressed at minimum energy below the Coulomb barrier, whereas at above barrier energy they show higher preformation probability. This variation in structure of fragmentation path across coulomb barrier in the IMF region is of great interest. We have

also estimated the magnitude of IMF & Fission contribution at the neck length parameter ΔR approximately half in magnitude as compared to that for evaporation residue (ERs) process. It is so, because our past experience with DCM based calculations suggests that ΔR for fission or IMF process is in general lower in magnitude than that for ER process. The DCM based calculations suggest that IMF and fission contribution come out to be 2.08×10^{-4} mb & 2.94×10^{-11} mb respectively.

In order to look out for fragmentation pattern and particularly the structural variation observed in IMF region, we have included the deformation effects to have better insight of the dynamics of $^{6}Li + {}^{90}Zr \rightarrow {}^{96}Tc^{*}$ reaction.

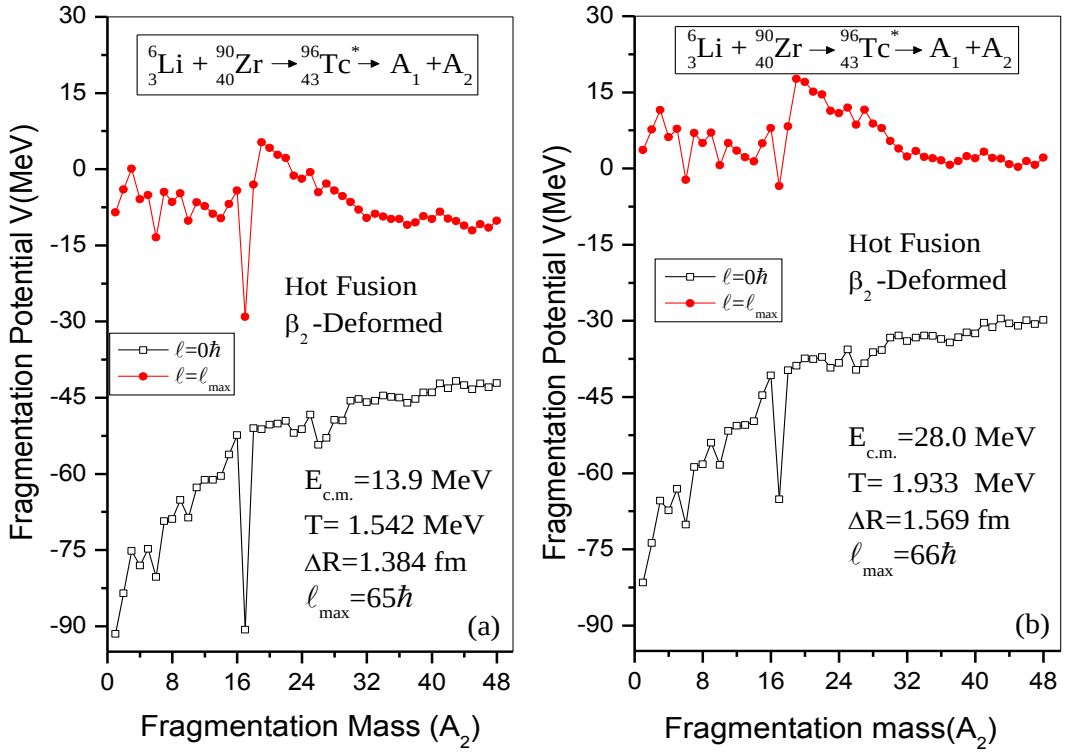

Fig. 3.3 *Fragmentation potential as a function of fragment mass (A_2) for β_2 deformed fragmentation at (a) $E_{c.m.}$ =13.9 MeV, (b) $E_{c.m.}$ =28.0 MeV.*

In order to study the role of deformation in the decay of $^{96}Tc^{*}$ system, we have carried out the calculations by taking quadrupole (β_2) deformations into account. Although

calculations have been done at all reported energies but we have shown fragmentation behavior only at extreme energies as depicted in following figure.

In Fig.3.3 with inclusion of deformations the minima at ^{17}B in fragmentation potential at both extreme energies shows the preference of these fragments. However, with its small penetrability, it does not contribute much towards the total cross-sections. From the figure it is clear that the potential energy surface is almost same at both minimum and maximum energy across the barrier. The neck-length parameter is found to increase with increase in energy as observed for spherical fragmentation. However, at minimum energy i.e. $E_{c.m.}$=13.9 MeV, ΔR value changes considerably from 0.780 fm to 1.384 fm while going from spherical to β_2 deformed choice of fragmentation. Whereas, at maximum energy, i.e. $E_{c.m.}$=28.0 MeV very slight change is observed in the magnitude of ΔR, being 1.526 fm for spherical and 1.569 fm for β_2 deformed choice.

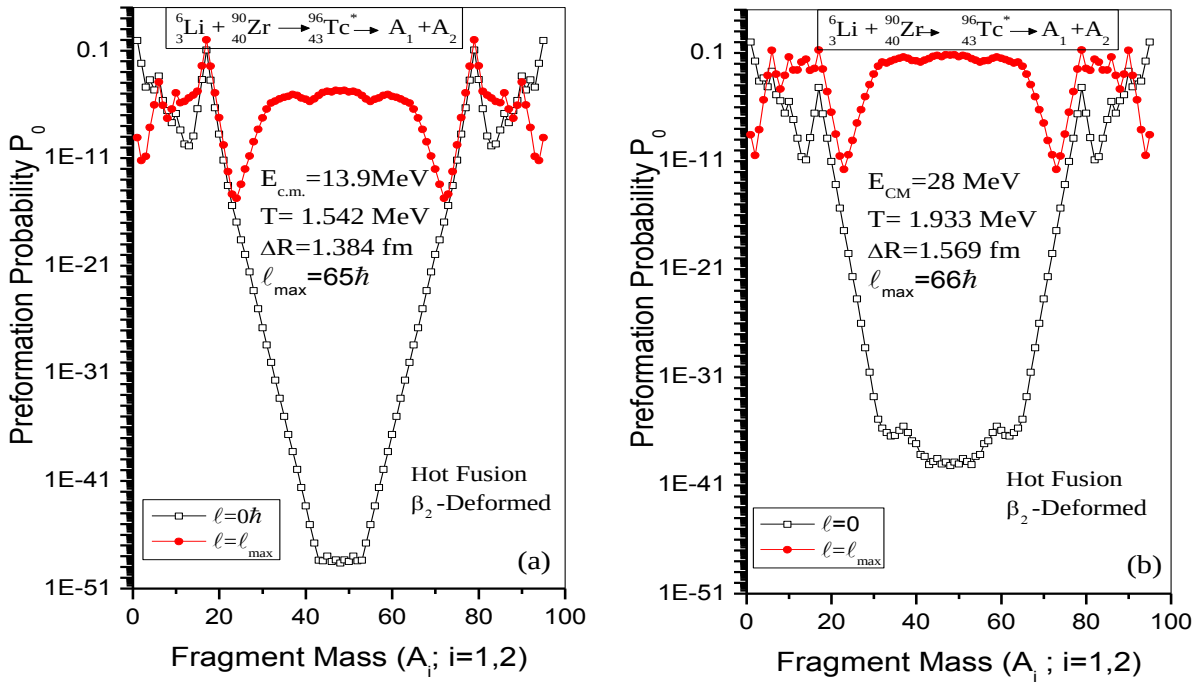

Fig.3.4 *Preformation probability as a function of fragment mass for β_2-deformations at (a) $E_{c.m.}$ =13.9 MeV and (b) $E_{c.m.}$ =28.0 MeV.*

By including β_2-deformation effects, the preformation probability is plotted at minimum and maximum ℓ-values at extreme energies across the barrier. With inclusion of β_2-deformation, a significant change is observed in the behavior of preformation probability while going from minimum to maximum energy. At $E_{c.m.}$=13.9 MeV, the structure of fragments at ℓ=0$\hbar$ is much steeper which otherwise become wider at highest energy i.e. $E_{c.m.}$=28.0 MeV. Also at ℓ= $\ell_{max,}$ the intermediate mass fragments dominate and have highest preformation probability as compared to other fragments at minimum energy. On the contrary, at highest energy the fission fragments start competing with IMF production.

Table 3.1*: The decay cross sections for evaporation residues ERs calculated using DCM for the $^{96}Tc^{*}$ nucleus formed in the $^{6}Li+^{90}Zr$ reaction with the inclusion of quadrupole deformation, at all $E_{c.m.}$ values and at ℓ_{max}~65ħ, compared with the experimental data.*

E_{lab} (MeV)	$E_{c.m.}$ (MeV)	ΔR(fm)	ℓ_{max} (ħ)	σ_{ER} (mb)	σ_{EXP} (mb)
29.9	28.0	1.569	66	773.58	778±37
24.9	23.3	1.529	65	510.88	510±24
20.9	19.6	1.500	66	231.52	230±11
18.9	17.7	1.464	65	115.00	114±7
17.9	16.8	1.452	65	62.10	63±4
16.9	15.8	1.433	65	27.02	27±2
15.9	14.9	1.406	65	6.13	6.3±0.6
14.9	13.9	1.384	65	1.37	1.3±0.2

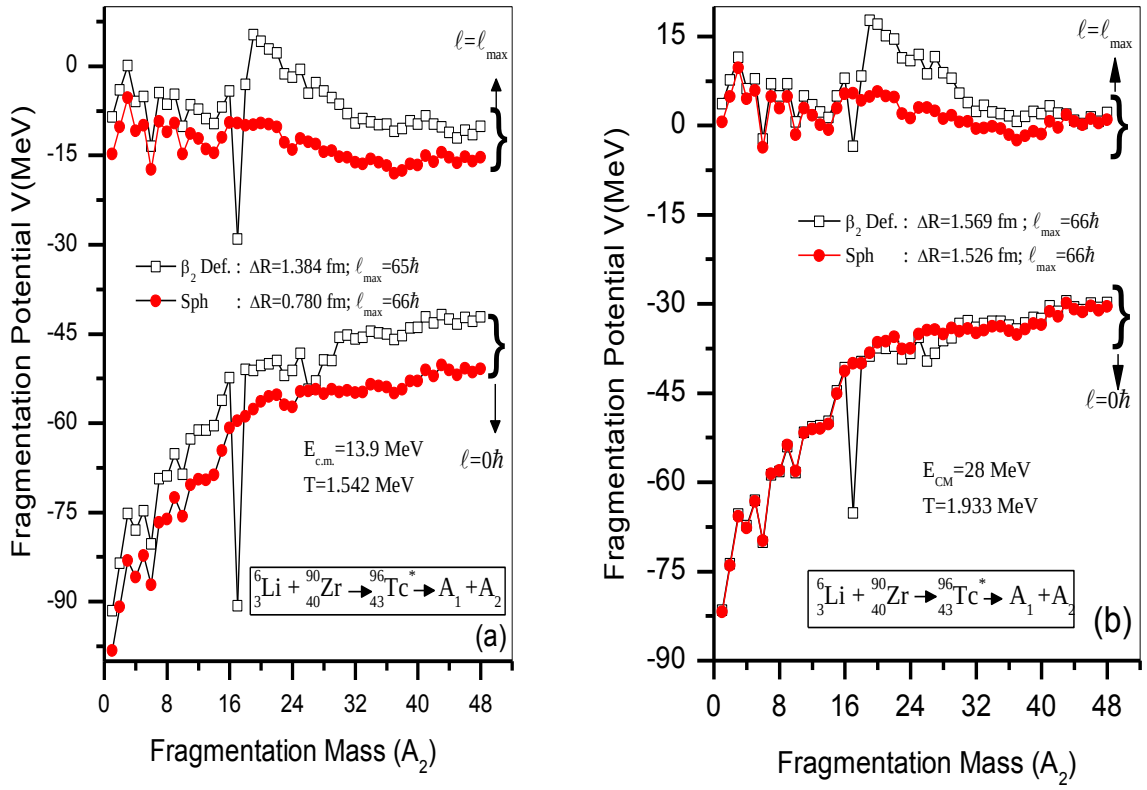

Fig. 3.5 *Comparison of fragmentation potential calculated using β_2-deformed fragmentation and spherical fragmentation at (a) $E_{c.m.}$=13.9 MeV and (b) $E_{c.m.}$=28.0 MeV*

The comparison of structural behavior of potential energy surfaces (PES) of spherical and quadrupole (β_2) deformed choice of fragmentation is shown in Fig. 3.5. As is clear from the figure, the role of deformation is prominent at both $\ell=0\hbar$ and $\ell=\ell_{max}$ values for minimum energy, $E_{c.m.}$=13.9 MeV whereas, at highest energy, $E_{c.m.}$=28.0 MeV the role of deformations is observed only at $\ell=\ell_{max}$. It is worth mentioning here that with inclusion of deformations, the barrier becomes shallow and barrier height decreases. Due to this the fusion probability increases for deformed fragmentation.

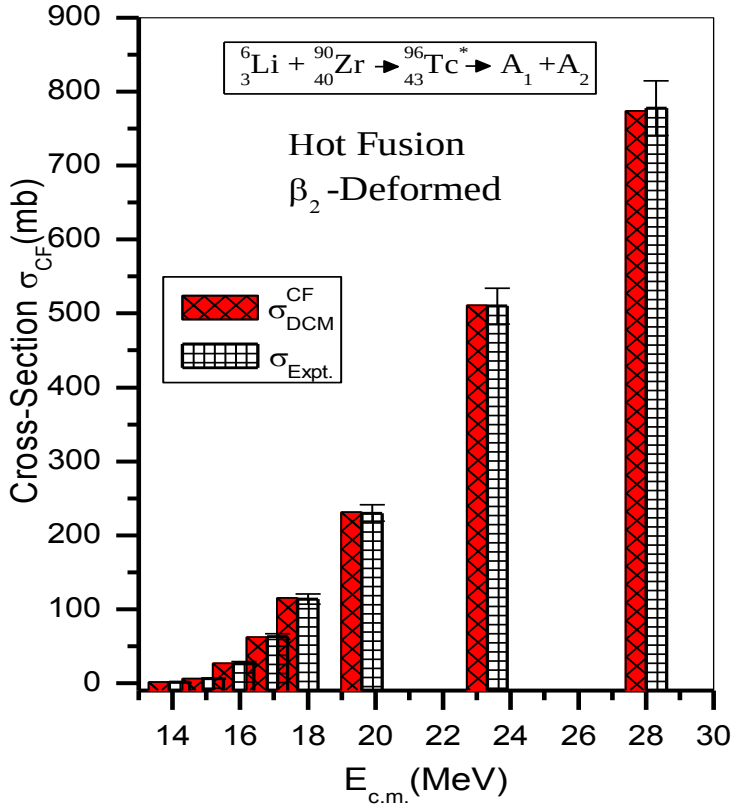

Fig. 3.6*: Variation of complete fusion cross-sections with $E_{c.m}$ for decay of $^{96}Tc^{*}$ in $^{6}_{3}Li + ^{90}_{40}Zr \rightarrow ^{96}_{43}Tc^{*}$ reaction.*

It must be noted that for this intermediate nucleus the main decay mode contributing towards cross-section is evaporation residues (ER) involving emission of 1n, 2n, 3n and 4H or 4n fragments. A comparative study of calculated DCM cross sections with experimental data showing contributions of ER is shown in Fig. 3.6. It may be noted that the evaporation residue channel is the only contributor towards complete fusion cross-sections. The evaporation residue cross-sections calculated using DCM is found to be in nice agreement with the experimental data of [1]. It is relevant to mention here that DCM supports the emission of evaporation residues in the decay of ^{96}Tc* nucleus formed in ^{6}Li induced reaction across the barrier.

The experiment carried out to study the decay cross sections formed in ^{6}Li+^{90}Zr → ^{96}Tc* reaction [1] shows that CF cross sections are suppressed by ~34%. This suppression is

associated with incomplete fusion process observed due to the break-up of loosely bound projectile ^{6}Li into two fragments, ^{2}H and ^{4}He. The measured total reaction cross-sections contain contribution of complete fusion and incomplete fusion (or α-transfer process).

$$\sigma_{\text{Reaction cross-section}} = \sigma_{\text{CF cross-section}} + \sigma_{\text{ICF cross-section}}$$

In framework of DCM we have carried out the calculations to address the ICF cross-sections obtained by subtracting the contribution of complete fusion cross-section from the total reaction cross-section. Based on these results, the contribution of ICF due to break-up of ^{6}Li projectile have been studied by considering the ^{4}He channel. In the framework of DCM the calculations for ICF have been done by applying relevant and necessary energy corrections [9] to obtain the energy of the new projectile (^{4}He) involved. In other words calculation has been done for $^{4}_{2}\text{He} + {}^{90}_{40}\text{Zr} \rightarrow {}^{94}_{42}\text{Mo}$ reaction with evaporation residues as the only decay channel.

Table 3.2: *The ICF (incomplete fusion) cross-sections calculated using DCM for the $^{94}Mo^{*}$ nucleus formed in the $^{4}He+^{90}Zr$ reaction with the inclusion of quadrupole deformation, at all $E_{c.m.}$ values and at ℓ_{max}~66ħ, compared with the experimental data.*

E_{lab} (MeV)	$E_{c.m.}$ (MeV)	ΔR(fm)	ℓ_{max} (ħ)	σ^{ICF}_{DCM} (mb)	σ^{ICF}_{EXP} (mb)
19.9	19.10	1.330	66	596.0	597.0
16.6	15.90	1.290	66	558.0	560.0
13.9	13.30	1.250	66	418.0	445.0
12.6	12.10	1.230	66	295.0	300.0
11.9	11.40	1.214	66	193.0	196.0
11.3	10.80	1.205	66	131.0	131.2
10.6	10.10	1.187	66	71.3	71.4
9.9	9.50	1.174	66	39.1	38.0

The calculations have been done by taking quadrupole deformations into account. Table 3.2 shows the variation of cross-section as a function of center of mass energy ($E_{c.m.}$). The DCM based results and the experimental cross-sections for incomplete fusion are in good agreement with each other. This shows that the DCM approach responds well to the reactions involving loosely bound nuclei having contribution of complete fusion (CF) as well as incomplete fusion (ICF).

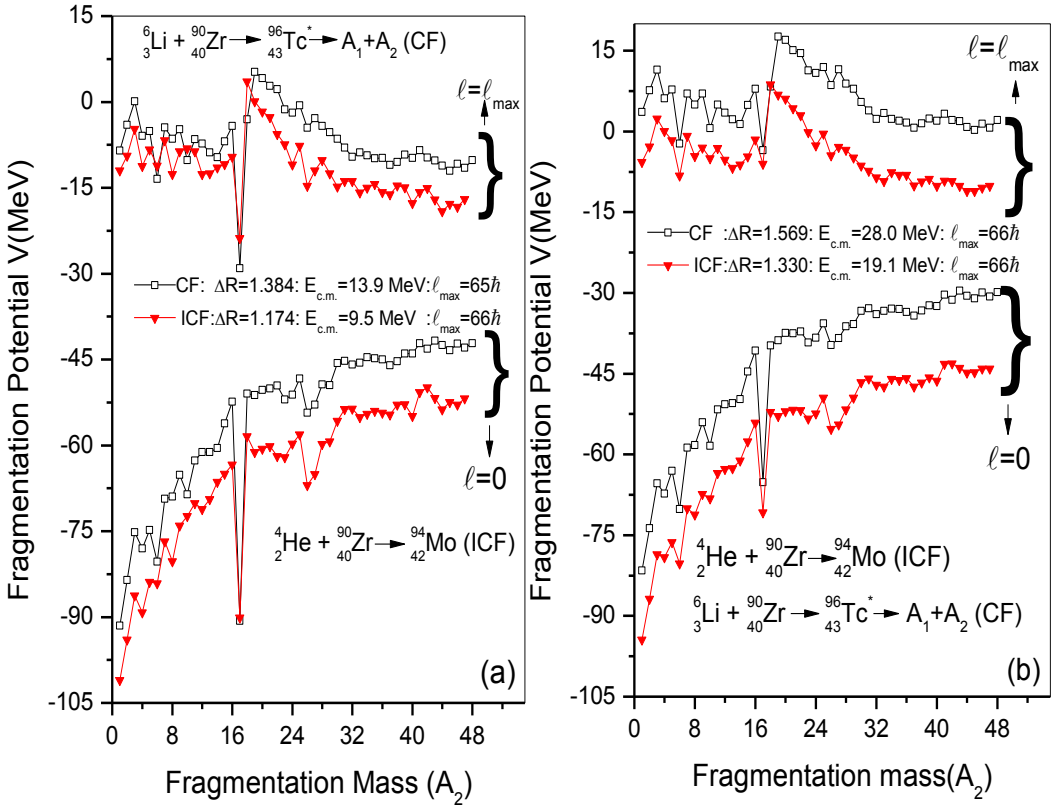

***Fig.3.7**: Comparison of CF and ICF based fragmentation potential as a function of fragment mass at (a) $E_{c.m.}^{CF}$ =13.9 MeV and $E_{c.m.}^{ICF}$=9.5 MeV and (b)$E_{c.m.}^{CF}$ =28.0 MeV and $E_{c.m.}^{ICF}$ =19.1 MeV for ICF.*

A comparison of the fragmentation potential of complete fusion (CF) and incomplete fusion (ICF) processes is shown in Fig. 3.7. From the figure it is observed that the

structural behavior of fragments in both the processes remains almost identical. However, the neck-length parameter involved in both these processes is different.

Fig. 3.8 shows the variation of neck-length parameter ΔR (only parameter of DCM) as a function of centre of mass energy $E_{c.m.}$ for complete fusion (CF) and incomplete fusion (ICF) processes. One may notice that independent of decay process the ΔR varies almost linearly as a function of incident energy. Also, the magnitude of ΔR is much higher for complete fusion (CF) process as compared to that for incomplete fusion (ICF). In context of chosen reaction this observation seems to suggest that the complete fusion (CF) occurs at relatively elongated neck as compared to ICF mechanism

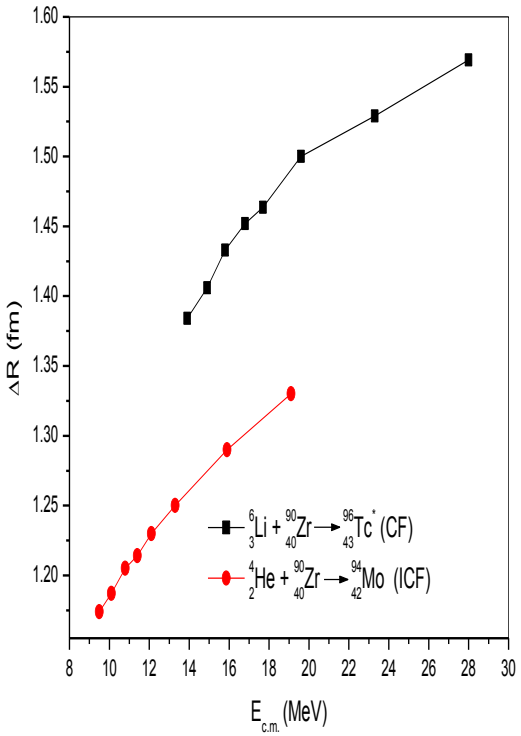

Fig 3.8: *Neck length parameter (ΔR) as a function of* $E_{c.m.}$ *for* $^{6}_{3}Li + ^{90}_{40}Zr \rightarrow ^{96}_{43}Tc^{*}$ *(CF) and* $^{4}_{2}He + ^{90}_{40}Zr \rightarrow ^{94}_{42}Mo$ *(ICF) reactions.*

In summary we have calculated the complete fusion cross-sections using DCM by using spherical as well as β_2-deformed fragmentation for the ^{6}Li + ^{90}Zr→^{96}Tc*. Structure of

Fragmentation potential remains almost identical for both β_2-deformed as well as for spherical choice of fragmentation. As ^{6}Li is loosely bound system thus it breaks in to α+d cluster which leads to fusion of α with ^{90}Zr and hence incomplete fusion cross-sections come into picture. The neck-length parameter (ΔR) increases with increase in energy for both, complete fusion as well as for incomplete fusion processes. DCM calculations suggest that CF process occurs at elongated neck as compared to ICF process in the ^{6}Li induced reaction across the coulomb barrier. As expected, deformations play significant role at lower energies as compared to higher ones.

References

[1] H. Kumawat, V. Jha, V. V. Parkar et al. Phys. Rev. C **86**, 024607, (2012).

[2] M. K. Sharma, G. Sawhney, R. K. Gupta, and W. Greiner, J.Phys. G: Nucl. Part . Phys. **38**, 105101, (2011); M. K. Sharma, G. Sawhney, S. Kanwar, and R. K. Gupta, Mod. Phys. Lett. A **25**, 2022, (2010).

[3] M. Kaur, R. Kumar, and M. K. Sharma, and M. K. Sharma, Phys. Rev. C **85**, 014609, (2012).

[4] B. B Singh, M K Sharma and R K Gupta, Phys. Rev. C **77**, 054613, (2008).

[5] K. Sandhu, M. K. Sharma, and R. K. Gupta, Phys. Rev. C **85**, 024604, (2012).

[6] R. Kumar and R.K. Gupta, Phys. Rev. C **79**, 034602, (2009).

[7] M. K. Sharma, G. Sawhney, S. Kanwar, R. K. Gupta, and W. Greiner, J. Phys. G: Nucl. Part. Phys. **38**, 055104, (2011); D. Jain, R. Kumar, M. K. Sharma, and R. K. Gupta, Phys. Rev. C **85**, 024615, (2012).

[8] M. Kaur, Manoj K. Sharma, And Raj K. Gupta, Phys. Rev. C **86**, 064610, (2012).

[9] G. Kaur and M. K. Sharma, Nucl. Phys. A **884**, 36, (2012).